Vanishing weekly hydropeaking cycles in American and Canadian rivers

Stephen J. Déry (sdery@unbc.ca)
University of Northern British Columbia https://orcid.org/0000-0002-3553-8949
Marco A. Hernández-Henríquez
University of Northern British Columbia
Tricia A. Stadnyk
University of Calgary https://orcid.org/0000-0002-2145-4963
Tara J. Troy
University of Victoria https://orcid.org/0000-0001-5366-0633

Research Article

Keywords: Canada, United States of America, Flow Regulation, Human Intervention, Hydropeaking, Hydropower, Streamflow

Posted Date: April 20th, 2021

DOI: https://doi.org/10.21203/rs.3.rs-441563/v1

Version of Record: A version of this preprint was published at Nature Communications on December 1st, 2021. See the published version at https://doi.org/10.1038/s41467-021-27465-4.

Vanishing weekly hydropeaking cycles in American and Canadian rivers

Stephen J. Déry[1,*], Marco A. Hernández-Henríquez[1], Tricia A. Stadnyk[2], and Tara J. Troy[3]

[1]Department of Geography, Earth and Environmental Sciences, University of Northern British Columbia, 3333 University Way, Prince George, British Columbia, V2N 4Z9, Canada

[2]Department of Geography, University of Calgary, Calgary, Alberta, T2N 1N4, Canada

[3]Department of Civil Engineering, University of Victoria, Victoria, British Columbia, V8W 2Y2, Canada

*Corresponding author: Stephen Déry (sdery@unbc.ca), ORCID # 0000-0002-3553-8949

Email address for Marco Hernández-Henríquez: hernandezhenriquez.m@gmail.com

Email address for Tricia Stadnyk: Tricia.Stadnyk@ucalgary.ca, ORCID # 0000-0002-2145-4963

Email address for Tara Troy: tjtroy@uvic.ca, ORCID # 0000-0001-5366-0633

CONFIDENTIAL MANUSCRIPT - FOR PEER REVIEW ONLY

31 March 2021

Running head: Vanishing weekly hydropeaking cycles in American and Canadian rivers

Keywords: Canada, United States of America, Flow Regulation, Human Intervention, Hydropeaking, Hydropower, Streamflow

Abstract

Sub-daily and weekly flow cycles termed 'hydropeaking' are common features in regulated rivers worldwide. Weekly flow periodicity arises from fluctuating hydropower demand and production tied to socioeconomic activity, typically with higher consumption during weekdays followed by reductions on weekends. Here, we propose a novel weekly hydropeaking index to quantify the 1920-2019 intensity and prevalence of weekly hydropeaking cycles at 400 sites across the United States of America and Canada. A robust weekly hydropeaking signal exists at 1.1% of sites starting in 1920, peaking at 17.0% in 1963, and diminishing to 3.2% in 2019, marking a 21st century decline in hydropeaking intensity. We propose this decline may be tied to recent, above-average precipitation, socioeconomic shifts, alternative energy production, and legislative and policy changes impacting water management in regulated systems. Vanishing weekly hydropeaking cycles may offset some of the prior deleterious ecohydrological impacts from hydropeaking in highly regulated rivers.

Introduction

In 2019, the United States of America (USA) and Canada generated a combined 674 TWh of hydroelectricity from a total 184 GW of installed capacity, ranking them with China and Brazil in the four largest global producers of hydroelectricity[1]. With the proliferation of dam and reservoir construction during the 20th and early 21st centuries[2, 3], many of the two countries' main rivers are now moderately or strongly affected by fragmentation, regulation and/or diversions[4-6]. With increasing demands for renewable sources of energy, additional generating capacity is being developed or planned across Canada. This includes the 1,100 MW Site C Dam on the Peace River in northeastern

British Columbia (BC), the 824 MW Muskrat Falls development on the lower Churchill River in Labrador, and the 695 MW Keeyask Generating Station on the Nelson River in northern Manitoba[1], with its first of seven units becoming operational in February 2021.

While overall demand for electricity continues to increase, consumption patterns vary depending on socioeconomic activity, short-term weather conditions, seasonal climate fluctuations and long-term climate trends[7, 8]. In the northern USA and Canada, the winter season usually incurs peak hydroelectric demand due to domestic, commercial and industrial heating and lighting requirements[9]. With climate change, winter cold waves subside while summer heat waves intensify[10, 11], shifting some of the demand from winter heating to summer cooling[12-14]. Apart from seasonality shifts, day-to-day activities influence hydroelectricity demand as well. Similar to many other industrialized countries, North American educational, industrial and commercial activity intensifies on weekdays (Monday through Friday) but abates on weekends, particularly on Sundays[9]. This weekly rhythm of socioeconomic activity can thus impact water retention and releases in regulated rivers[15]. These rapid, frequent and periodic flow fluctuations downstream of regulation points are commonly termed ‘hydropeaking’ events and are known to disrupt a range of ecohydrological processes[16, 17]. Yet the characteristics and trends in weekly hydropeaking cycles due to daily variation in hydropower demands remain largely unknown. This is despite the general availability of discharge data at a daily time scale and the distinct weekly rhythm of socioeconomic activity including hydropower production, and hence water releases in regulated waterways, which impact ecohydrological processes.

To address that knowledge gap and a demand for global attention to hydropeaking rivers[18], we assess here the prevalence of weekly hydropeaking cycles for 400 gauging sites along rivers of the USA and Canada spanning a wide range of basin characteristics, regulation, hydrological and climatic regimes. Specifically, we develop a scale-independent and dynamic weekly hydropeaking index (WHI) with both time and frequency domain terms, allowing quantification of weekly flow periodicity. Application of the novel WHI to 1920-2019 time series of river discharge provides evidence of vanishing weekly hydropeaking cycles in many regulated rivers of the USA and Canada with the 2010s comparable to the 1920s for hydropeaking prevalence. We conclude that increased commercial and industrial activity on weekends, a shift towards other modes of energy production, policy changes altering water management practices, electrical grid interconnectivity and deregulation of electricity generation, plus a relatively wet decade in the 2010s are contributing factors to waning weekly hydropeaking cycles.

Results

Overall WHI statistics. The 1980-2019 mean, median, and standard deviation of WHI for the 400 sites reach 0.097, 0.005 and 1.115, respectively (Supplementary Table 1). An application of the Shapiro-Wilk test to the WHI data suggests the distribution is not Gaussian ($W = 0.974$, $p = 1.32 \times 10^{-6}$, $n = 400$); yet, the low skewness (0.157) and excess kurtosis (0.754) along with a Cullen and Frey graph (Supplementary Fig. 1) infer a reasonable fit. Twenty-five sites attain a mean annual WHI ≥ 2.0 for 1980-2019 with another 49 sites achieving WHI ≥ 1.0. A list of sites with the top ten ranking WHI values reveals their wide regional distribution with foci in the Chattahoochee, Colorado, Columbia, Great Lakes-St. Lawrence, Nelson and upper Tennessee drainage basins

(Table 1), all of which are heavily dammed. The Chattahoochee River at Buford Dam claims the top WHI score of 3.299 while BC's Stuart River shows the lowest score of -3.469. Some highly regulated systems such as Manitoba's Burntwood River, which funnels water diverted from the Churchill River into the Nelson River, exhibit large negative WHI values (-1.892) as Notigi (the upstream point of regulation) is a control structure for a large reservoir operated in a longer term (e.g., seasonal) manner. Similarly, while several large dams impound the Missouri River, they are managed not only for hydropower production but also for flood control, irrigation, navigation and recreational values. As such, the three sites along the Missouri River used in this study exhibit an average WHI = -0.492 revealing an absence of significant weekly hydropeaking cycles.

Spatial analyses. A map of the 1980-2019 WHI values reveals that weekly hydropeaking rivers abound across the USA and Canada. Clusters of high WHI values emerge in the Alabama, Chattahoochee, and Tennessee river basins of the southeastern USA, in waterways draining the Ozark Mountains, the Colorado River and in northern Ontario rivers draining into the Great Lakes (Fig. 1). The Columbia River has several major points of regulation (WHI ≥ 1.5) from its headwaters in BC to its outlet in the Pacific Ocean. Highly hydropeaking sites (WHI ≥ 2.0) appear in both small (e.g., Alberta's Kananaskis River, A = 899 km^2) and large (Manitoba's Nelson River, A = 1.1 × 10^6 km^2) systems. In contrast to their adjacent regulated rivers, free-flowing rivers of northern Canada, particularly those draining into Hudson Bay, exhibit large, negative WHI values. These unregulated rivers manifest strong annual cycles dominated by snowmelt-driven freshets and contain large natural storage capacity in the form of

extensive lakes, ponds and wetlands. Free-flowing, pluvial rivers of the southeastern USA (e.g. the Choctawhatchee, Ogeechee, Pascagoula, Satilla and Suwanee rivers) also exhibit negative, albeit > -1.5, WHI scores. WHI values diminish moving downstream from a point of regulation. For instance, WHI = 1.437 on the Peace River just downstream of BC's WAC Bennett and Peace Canyon dams where minimum flows arise on weekends; 400 km downstream from the dams[19], however, WHI declines to 0.929 at the community of Peace River in Alberta where minimum flows occur on Mondays/Tuesdays, indicating a 2-day delay in signal propagation. A cascade of dams and reservoirs can amplify or sustain the hydropeaking signals along waterways (e.g., the Colorado, Columbia, and Tennessee rivers) or attenuate them (e.g., Ottawa River).

Sites with high values of WHI (≥ 1.5) also show a preponderance of flow reductions on the weekends (Saturdays/Sundays) as identified by the larger symbols in Fig. 1. Of the 44 sites with WHI ≥ 1.5, 39 experience the two consecutive days with low flows on weekends. In contrast, sites with negative WHI values show a range of low flow days with no distinct pattern emerging. No less than 30.8% of all sites used in this study exhibit low flows on Saturdays/Sundays, more than twice the expected value (Fig. 2). This disproportionate amount of weekend low flows occurs mainly in hydropeaking rivers (WHI > 0). Weekday combinations show frequencies at, or lower than, the expected value with the Friday/Saturday sequence appearing at only 6.0% of sites. A Chi-Square test applied to the frequency of two consecutive low flow days reveals that the results differ significantly from the expected value of 0.143 ($\chi^2 = 109.95$, $p < 2.2 \times 10^{-16}$, $n = 7$ with six degrees of freedom). The mean WHI equals 0.292 for 123 sites with

low flows on weekends while it remains near zero or slightly negative for the six other two-day combinations. The distribution of mean WHI for the two-day combinations differs significantly from a uniform distribution based on a Chi-Square test ($\chi^2 = 8.43$, $p = 0.05$ based on 10,000 replicates with $n = 7$).

Temporal evolution and trend analysis. The temporal evolution of the mean and median WHI shows a rapid increase in hydropeaking intensity from the 1920s to the 1950s at which point they level off and fluctuate near zero (Supplementary Fig. 2). Starting in the 1990s, though, there is a gradual decline in both the mean and median WHI values with a return in the 2010s to statistics first seen in the 1930s (largely pre-regulation), a pattern observed both in the USA and Canada (not shown). The discharge-weighted WHI_Q emphasizes the increasing volumes of regulated flows starting from the 1920s through the 1980s; however, WHI_Q also declines markedly thereafter into the 21st century. In 1920, only 1.1% of available sites rank in the top decile of 1920-2019 WHI values (WHI ≥ 2.021). This fraction peaks at 17.0% of available sites in 1963 but thereafter diminishes consistently. In 2000, 50 or 13.2% of available sites score in the top decile of 1920-2019 WHI values but these counts fall precipitously to just 12 or 3.2% of the available sites by 2019, marking a 21st century declining pattern in weekly hydropeaking intensity. Trend analysis applied to the overall mean annual WHI reveals a statistically-significant decline of -0.40 over 1980-2019 (Supplementary Fig. 3). These temporal results, however, rely on the availability of discharge data, as the record length averages 78.4 years, ranging from a minimum of 24 years at one site to a full century at 87 sites (Supplementary Fig. 4). The number of available sites increases steadily from 1920 into the early 1990s and peaks at 393 sites

in 1985 and 1992 but then declines to 373 sites by 1996 thereafter averaging 383±6 sites until 2019. Notable gaps appear in the discharge records starting in the 1990s, particularly for regulated rivers in Ontario and Québec; however, adjusting the time series of mean annual WHI for unavailable sites reveals little difference in the overall pattern and trend of WHI during 1980-2019 (Supplementary Fig. 3).

Data availability also factors in the appraisal of the decadal evolution of hydropeaking intensity across the USA and Canada (Fig. 3a-j). Nevertheless, this shows the gradual inception of hydropeaking cycles during the 1920s and 1930s, particularly in the north-central, northeastern, and southeastern USA and in northern Ontario. The 1940s show an expansion of weekly hydropeaking rivers into the western USA including within the Colorado, Columbia and Sacramento river basins. The 1940s and 1950s mark an intensification of regulation in the Tennessee and Alabama river basins as well as rivers of northern Ontario draining to Lakes Superior and Huron. A pronounced expansion and amplification of the hydropeaking signal appears in the 1960s, particularly across the Great Lakes-St. Lawrence river basin in Ontario and Québec. Some stabilization of the hydropeaking pattern marks the 1970s but a resurgence follows in the 1980s and 1990s when additional hydropeaking rivers emerge in western Canada. The 2000s retain a wide distribution of hydropeaking rivers across both countries; yet, by the 2010s, the number of highly hydropeaking rivers diminishes considerably, particularly in parts of the Great Lakes-St. Lawrence and Tennessee river basins. The decadal distribution of the 10 WHI bins (Fig. 3k) further highlights the peak fraction of sites with WHI ≥ 1.5 attained in the 1960s (19.6%), with nearly matching minimum values in the 1920s

187 (6.8%) and 2010s (6.7%). After the 1960s, there is a steady decline in the relative
188 number of sites with low flows either on the Saturday/Sunday or Sunday/Monday
189 combinations, indicating waning differences between weekday and weekend flows
190 across the USA and Canada (Fig. 3l).

191 The temporal evolution of the annual maximum WHI value shows a rapid increase from
192 ~3.0 in the 1920s to > 4.0 in the 1930s onward (Supplementary Fig. 2d). Annual peak
193 WHI values > 4.0 are generally sustained for the remainder of the 20th century but then
194 fall below that threshold starting in 2003 until 2019. The peak WHI value each year over
195 the study period is distributed among 19 sites, with the Winnipeg River at the outlet of
196 the Lake of the Woods capturing the top spot 12 times in the 1920s to early 1960s
197 (Supplementary Fig. 5). The Colorado River at Hoover Dam dominates the list 25 times
198 between the 1940s into the early 1980s. From the 1960s to 2010s, the Chattahoochee
199 River at Buford Dam ranks first 12 times while in the 1990s and 2000s, the Montreal
200 River that drains to Lake Superior tops the list 10 times. The overall maximum WHI
201 score of 4.587 arises in 1961 at the Winnipeg River at the outlet of Lake of the Woods.

202

203 Further statistical analysis reveals an abundance of strong, negative WHI trends
204 interspersed with positive ones for the 380 sites with $n_y \geq 30$ years over 1980-2019 (Fig.
205 4). A total of 104 sites show locally statistically-significant ($p < 0.05$) declines in WHI
206 while 26 show locally statistically-significant inclines. Of the 130 locally-significant
207 trends, 81 remain globally significant. Significant negative WHI trends abound in the
208 southeastern and northeastern USA, the Great Lakes-St. Lawrence basin, and the

Pacific Northwest while a cluster of positive trends arises in Québec's Saguenay watershed. While regulated rivers of Newfoundland show increasing WHI values, their unregulated counterparts show similar tendencies. Similarly, in New Brunswick, the regulated St. John River shows a decreasing trend in WHI while the proximal, unregulated Southwest Miramichi River shows an increasing trend. Sixty-four percent of the locally-significant WHI trends arise in hydropeaking rivers (WHI > 0) with fewer locally-significant trends in non-hydropeaking rivers (WHI < 0; Supplementary Fig. 6).

Interannual and interdecadal variability. Water management practices and climate variability, among other factors, yield significant interannual variation in hydropeaking intensity. For example, the Colorado River at Lees Ferry shows marked declines in WHI during high flow years (Supplementary Fig. 7a). Indeed, heavy precipitation during strong El Niño events in the early 1980s induced high flows in the Colorado River including at Lees Ferry. Due to the unusually wet weather, the bypass tubes and spillway at Glen Canyon Dam were used to release additional water downstream, thereby moderating hydropeaking signals from 1983 to 1986[20]. Similar declines in WHI appear in 1997 and 2011 when flows exceed the recent annual average. Computing the Pearson correlation coefficient between the 1980-2019 annual river discharge and the corresponding WHI yields 81 statistically-significant negative correlations and only 16 statistically-significant positive correlations (Supplementary Fig. 7b). Thus high flows over extended periods attenuate weekly periodicity even in heavily regulated rivers such as the Colorado.

This analysis suggests that sustained wet periods may attenuate hydropeaking intensity while dry periods may accentuate it. Binned distributions of decadal standardized anomalies in river discharge reveal the contrasting dry 1930s vs. the wet 1970s, the latter coinciding with a suppression of hydropeaking across the USA and Canada (Supplementary Fig. 8). Yet, while the 2010s experienced relatively high flows, 6.7% of sites have WHI ≥ 1.5 whereas in the similarly wet 1990s, 15.6% of sites achieve WHI ≥ 1.5. Of 20 sites with large (> 1), positive standardized discharge anomalies during the 2010s, only three (the Betsiamites, La Grande and Nelson rivers) have WHI > 1, which are likely more in response to enhanced diverted flows rather than high precipitation. Thus it is unlikely interdecadal climate variations alone account for recent WHI declines.

Dispersion of daily flows. Apart from climate variations, changes in day-of-the-week flows may influence WHI trends. Sites with WHI > 0 generally observe greater dispersion of day-of-the-week flows although pluvial and intermittent rivers, particularly in the southern USA, also experience greater day-to-day flow variations (Supplementary Fig. 9a). A trend analysis reveals significant declines in the dispersion of flows across the seven days of the week, concomitant with diminishing WHI values from 1980 to 2019 (Supplementary Fig. 9b). As an example, an abrupt reduction in dispersion of day-of-the-week flows in Labrador's Churchill River appears in 1997 and is then sustained, suggesting factors other than climate variations are altering daily flows (Supplementary Fig. 10).

Discussion

Possible factors leading to recent WHI declines. The recent decline in weekly hydropeaking cycles in the USA and Canada emerges as a key finding in this study. Several possible factors may be contributing to this general pattern observed over the study area. Firstly, hydropower demand, production and consumption may have shifted in recent years, thereby diminishing differences between weekdays vs. weekends. For instance, there has been a gradual shift towards more commercial (including e-commerce) and industrial activity on weekends that could alter the weekly discharge patterns in regulated rivers[21, 22]. A shifting manufacturing sector, globalization, and lifestyle changes are all socioeconomic factors modifying electricity demand. Another possible factor is the development and expansion of other modes of energy production such as dispatchable combustion turbines and non-dispatchable solar and wind energy. Solar and wind energy production activate during favourable weather conditions with hydropower otherwise matching the demand, which may disrupt the typical weekly pattern in regulated flows. Regulatory bodies and changing governmental policies may also be altering how utilities manage regulated waterways. Indeed, there is renewed interest for environmental, ecological and cultural (e.g., from a First Nations perspective) flows in human-influenced systems, with emerging regulations and policies supporting their implementation[23]. For instance, regulatory changes in the operation of the Prickett hydroelectric facility from a peaking to run-of-river site to assist spawning lake sturgeon[24] induced a significant WHI decline (of -0.216 decade^{-1}) along the Sturgeon River in the upper peninsula of Michigan starting in the 1990s. Indeed,

276 changes in operation away from peaking hydropower generating stations, whether
277 mandated or voluntary, could influence hydropeaking patterns.
278
279 Additionally, the increasing interconnectivity of the North American power grid,
280 deregulation, and centralization of electricity dispatching may further contribute to a
281 recent reduction of hydropeaking intensity. Finally, climate variations may also play a
282 role in hydropower production as wet periods may require greater spillage of water from
283 reservoirs thereby diminishing hydropeaking intensity. The relatively wet climate of the
284 2010s could account for part of the recent declines in WHI across the USA and Canada.
285 Thus a combination of factors including changing hydropower demand patterns tied to
286 lifestyle factors and socioeconomic activity, the emergence of alternative modes of
287 energy production plus power grid interconnectivity, implementation of regulations and
288 policies, and climate variations may be influencing the day-to-day hydrology of many
289 regulated waterways across the USA and Canada.
290
291 **Spatio-temporal patterns within and across jurisdictions.** Given the vast territory of
292 the USA and Canada, their waterways often drain multiple jurisdictions including
293 international transboundary watersheds (e.g., the Rio Grande, Great Lakes-St.
294 Lawrence, Winnipeg and Columbia rivers). Regional water authorities, inter-
295 jurisdictional water boards, federal, provincial, and state legislation, and international
296 water treaties and commissions all affect how waterways are managed. Furthermore,
297 synchronous inter-jurisdictional power grids (e.g., interconnections) can also affect
298 hydropower generation and hence regulated flows, leading to distinct spatio-temporal

patterns in hydropeaking intensity. Decadal maps of WHI values reveal the progression of weekly hydropeaking systems from the eastern and central USA to the Pacific Northwest in the 1960s when development in the Columbia River Basin expanded rapidly. The international Columbia River Treaty implemented in 1961 led to the construction of three major dams along the Columbia River (Duncan, Keenleyside and Mica Dams in Canada) plus another on the Kootenai River (Libby Dam in the USA)[25]. These dams and generating stations expanded the presence of hydropeaking cycles from the lower to the upper Columbia Basin in the 1970s and 1980s (Fig. 3). As such, regulation in the Canadian portion of the Columbia Basin now leads to downstream propagation of hydropeaking into the northern USA where it is regenerated at multiple points of regulation including Grand Coulee Dam and the Dalles.

Another noticeable pattern in the decadal results is the WHI decline in many rivers of southern Québec in the 1970s and 1980s. As the 5,428 MW Churchill Falls generating station in Labrador came online in late 1971 (with hydropower sold mainly to the provincial utility Hydro-Québec)[26], followed a decade later by the 17,418 MW James Bay Hydroelectric Complex in northern Québec[15], a northward shift in hydropower generation abated the weekly hydropeaking cycles in more southern waterways. Simultaneous reductions in WHI in the northeastern USA (e.g., Hudson and Connecticut Rivers) may also be tied to transboundary power grid interconnections and Hydro-Québec's large export capacity (7,974 MW in 2019[27]). Similar to regional climate trends[28], synchronous power grids thus have the capacity to shift the intensity of hydropeaking signals 1000s of kms away from points where hydropower is consumed,

thereby creating *hydropeaking teleconnections* with potential for far-reaching social and ecohydrological effects.

Ecohydrological implications. Ecohydrological impacts of hydropeaking are site-specific and may include rapid changes in water temperature (i.e., 'thermo-peaking'), increases in soil erosion and suspended matter, and habitat degradation, which affect ecosystems, reduce species abundance, and limit biodiversity (e.g., fish, riparian plants, macroinvertebrates)[16, 29, 30]. Across the USA and southern Canada, hydropeaking emerged relatively early in the 20th century with the proliferation of dams and flow regulation in these regions. Starting in the 1960s, hydropower infrastructure expanded northwards into regions previously devoid of any significant flow regulation and hydropeaking. This includes major waterways like BC's Peace River, Manitoba's Nelson River, Ontario's Moose and Abitibi rivers, and Québec's La Grande Rivière. On these systems, major dams and reservoirs were built from the 1960s to early 1980s, vastly expanding the northern reach of hydropeaking rivers (Supplementary Fig. 11). This shifted potential ecohydrological impacts of hydropeaking to areas also undergoing rapid climate change through Arctic amplification of global warming[31]. As such, sub-Arctic species of fish (e.g., brook trout, lake sturgeon, northern pike, and walleye), insects and riparian plants may now be exposed to the cumulative impacts of these environmental stressors[17]. Additionally, winter frazil ice production and ice jams may be precipitated and accentuated downstream of hydroelectric facilities with persistent hydropeaking signals such as in the Peace River[19].

Despite their recent northward expansion, weekly hydropeaking cycles are generally waning across the USA and southern Canada, suggesting a 21st century *hydropeaking recovery* in some of these river systems. Indeed, prior ecohydrological impacts of hydropeaking may be partially offset, benefiting local biota and ecosystem biodiversity[32]. For instance, recovery of lake sturgeon in the northern peninsula of Michigan demonstrates some of the benefits of shifting away from peaking hydropower operations[24]. This is particularly important as evidence is also mounting that hydropeaking influences aquatic species in rivers of Canada[33-36]. Other aspects of flow regulation, such as sub-daily flow fluctuations and associated ramping up and down cycles not investigated in this study, may negate this hydropeaking recovery[16, 17]. Additional research is thus needed to explore hydropeaking cycles at other temporal scales to establish their site-specific ecohydrological impacts.

Advantages and limitations of the WHI relative to other metrics. The proposed index to infer weekly hydropeaking signals provides a complementary metric to those developed in other studies[5, 37, 38]. Advantages of our approach include its scale independence, dynamic response, and relatively simple implementation. The WHI can be applied from small ($< 1 \times 10^3$ km^2) to large ($> 1 \times 10^6$ km^2) river basins with available daily discharge data (whether observed, reconstructed or simulated). The WHI responds to interannual variability in climate (e.g., wet/dry periods), changes in water management practices and policies, commissioning of new hydroelectric facilities or decommissioning of old ones, and other factors that affect flows. The use of daily discharge data also avoids the need for extensive databases on dams, reservoirs and

368 other infrastructure that influence flows. Its possible implementation for short-term flow
369 predictions emerges as another distinct advantage of the WHI. As an example, a
370 running value of the WHI can be computed on the past year's daily flows and used to
371 infer the possible deviations in daily flows over a given week based on recent historical
372 patterns. Its computational simplicity, coded in our study in Fortran, allows processing of
373 results for the 400 sites in < 2.5 minutes. As such, it is feasible to implement a version
374 of the code for short-term flow predictions so long as up-to-date daily flow records
375 remain available. It would also be relatively straightforward to adapt the code to explore
376 sub-daily hydropeaking cycles[9] if appropriate discharge data are available.
377
378 One challenge in implementing the WHI is access to daily discharge records. While
379 considerable gauging stations exist in most of the USA and southern Canada, other
380 waterways are not necessarily well monitored. A late 20th century decline in hydrometric
381 stations due to budget restraints[39] and the Water Survey of Canada's curtailment of
382 data collection combined with stricter quality standards from third parties have
383 exacerbated hydrological data accessibility. As well, private industry and government-
384 owned corporations often record discharge at or near their hydroelectric facilities but
385 may consider these data as sensitive such that they are not released publicly. Thus,
386 acquisition of daily discharge data in regulated systems, particularly as the number of
387 small, private firms operating run-of-river hydroelectric facilities expands[3], yields a
388 distinct challenge in accessing flow data. Therefore, remote sensing[40], data
389 reconstructions (e.g. from statistical models or machine learning methods[41]) and

numerical simulations that incorporate regulation[42] are key in filling spatio-temporal gaps where and when *in situ* observations are lacking.

Concluding remarks. As hydropower generation and infrastructure development continues to expand across the USA and Canada, it is important to establish how water management practices affect downstream river flows and ecosystems. A common feature in regulated rivers are discharge periodicities associated with hydropower production ebbs and flows including weekly cycles. In this study, a new measure of this weekly rhythm in flows, the weekly hydropeaking index (WHI), is formulated and applied to 400 sites over parts of North America. Our findings reveal vanishing weekly hydropeaking cycles across the USA and Canada in the 2010s, suggesting diminishing differences between discharge on weekends vs. weekdays. Factors possibly yielding this result include increased commercial and industrial activity on weekends, a shift towards other modes of energy production during peak demand hours or days, and policy changes altering water management practices including for ecological and environmental flows. This reduction in weekly hydropeaking also may benefit aquatic species, insects and riparian vegetation that otherwise are susceptible to rapid shifts in flows and water levels. Future efforts should therefore establish the ecohydrological implications of waning hydropeaking cycles. The application of the WHI to other regions over the globe would provide broader perspectives on the commonality of this feature in regulated rivers.

Methods

Study area. The USA and Canada harbor abundant freshwater resources that include some of the world's largest rivers (by annual volumetric flows) including the Mississippi, St. Lawrence, Mackenzie, Ohio and Columbia rivers[43]. Many of these rivers and/or their tributaries have been impounded for hydropower generation, flood control, irrigation, potable water supply, navigation and recreation, leading to fragmented river networks and regulated flows[4, 6]. Indeed, numerous dams have been built across the USA and Canada in the 20th and early 21st centuries[2, 3]. While many dams in North America have multiple purposes, hydropower generation remains a principal function. Distinct weekly patterns mark hydropower production except perhaps at run-of-river facilities and those supplying industries continuously in operation such as aluminum smelters or pulp and paper mills[8, 9]. As such, this study focuses on both regulated and unregulated waterways of the USA and Canada to explore the prevalence and intensity of weekly periodicity in discharge.

Site selection. A total of 400 sites across the USA and Canada ranging 480-1,805,222 km^2 in gauged area (*A*), 25-60°N in latitude, 54-132°W in longitude, and 0.11-268.28 km^3 in mean annual discharge are selected for this study (Supplementary Fig. 12 and Supplementary Table 2). A primary site selection criterion is discharge data availability for ≥ 24 years between 1920-2019, with ≥ 14 years during the focus period of 1980-2019. The chosen sites span a wide range of hydrological regimes from pluvial rivers in warmer climates (e.g., BC's Yakoun River) to nival and glacial systems at higher elevations or latitudes in cooler climates (e.g., BC's Lillooet River)[44]. Thus, the study area spans regions with little to no snowmelt where sub-annual scales govern temporal

variability while others are mainly snowmelt-driven with predominant annual cycles[45]. The database also includes intermittent streams in warmer, drier climates such as California's Santa Ana River and Arizona's Little Colorado River. Regulated and unregulated rivers are selected (using guidance from Benke and Cushing[43]) to allow comparisons between sites. Some sites such as Lees Ferry on the Colorado River include extended records that cover pre- and post-regulation effects on flows.

Data. Data and metadata (station ID, gauge coordinates, and gauged area) are extracted from various sources including publicly accessible databases maintained by federal, provincial and state agencies in addition to proprietary data from private industry, government-owned utilities and international commissions. For most unregulated rivers, daily discharge data are sourced partly from the Water Survey of Canada's Hydrometric Database (HYDAT), the Centre d'Expertise Hydrique du Québec (CEHQ) and the United States Geological Survey (USGS). For regulated rivers, though, daily discharge data are not necessarily available from these sources or other public repositories as they are partially or entirely collected, quality controlled and archived by government-controlled utilities or private industry (see Supplementary Tables 2 and 3). This includes: Nalcor Energy for the Salmon and Exploits rivers plus the Churchill Falls (Labrador) Corporation Limited for the Churchill River at Churchill Falls Powerhouse in Newfoundland and Labrador; NB Power for the St. John River in New Brunswick; Rio Tinto for the Kemano Powerhouse in BC and the Saguenay and Péribonca rivers in Québec; Hydro-Québec for La Grande Rivière, Betsiamites, Manicouagan, des Outaouais, des Outardes and St-Maurice rivers; Evolugen by Brookfield Renewable for the Coulonge, Lièvre, and Noire rivers in Québec and Mississagi and Aux Sables rivers

458 in Ontario; Ontario Power Generation for the Abitibi, English, Kaministiquia,
459 Madawaska, Mattagami (tributary to the Moose River), Montreal and Ottawa rivers; H2O
460 Power for the Abitibi River; Manitoba Hydro for the Nelson and Winnipeg rivers;
461 Transalta for the North Saskatchewan and Kananaskis rivers; and BC Hydro for the
462 Columbia River at Mica Dam. Additional data for gauges along the Rio Grande on the
463 border between the USA and Mexico and the Pecos River are provided by the
464 International Boundary and Water Commission. Data at six sites in the Tennessee River
465 Basin are provided by the Tennessee Valley Authority. Recent records of daily
466 discharge from the US Bureau of Reclamation supplement those from the USGS for
467 sites on the Colorado and upper Rio Grande rivers. Finally, the 1 October to 31
468 December 2019 daily discharge data for the Snake River at Hells Canyon Dam are
469 sourced from Idaho Power. Potential errors associated with discharge measurements
470 and implications to our results are discussed in the Supplementary Methods.

471 **Time series construction.** The overall study period spans 1 January 1920 to 31
472 December 2019 for which at least partial, extended (≥ 24 years) records of daily
473 discharge are available at all sites. Time series of daily streamflow (in $m^3 s^{-1}$) are
474 constructed based on data availability for each site of interest (Supplementary Table 2)
475 and follows Déry et al.[46] in its approach. Daily discharge data sourced from the USGS,
476 US Bureau of Reclamation, Tennessee Valley Authority, Idaho Power, Nalcor Energy
477 (Exploits River) and NB Power are converted to metric units prior to analysis. For
478 several waterways (e.g., the Nelson and Saguenay Rivers), data furthest downstream
479 are first used, but when unavailable (prior to construction of dams and hydroelectric
480 facilities), are replaced with those from the closest upstream gauging station while

adjusting the data for the missing contributing area as necessary[46, 47]. Gaps are in-filled with the mean daily discharge over the period of record; however, any calendar year with ≥ 10% missing records is excluded from analysis. Supplementary Table 2 lists the percentage of in-filled data at each site (average: 0.02%, maximum: 0.55%) omitting years when ≥10% of the data remain unavailable. Uncertainty in the results associated with data homogeneity and the gap-filling strategy is evaluated and discussed in the Supplementary Methods.

Development of the WHI. Various approaches are commonly used to explore flow alterations in regulated rivers including comparisons of hydrographs pre- and post-regulation[9, 48, 49], trends in peak and/or low flows[50] or of naturalized versus observed (regulated) flows[51-53]. A broader approach employs a set of multiple (up to 33) indicators of hydrologic alteration (IHA) to quantify changes over the water year arising from regulation[54-56]. Another method combines hydrological data, reservoir information and a database of large dams in developing river regulation and fragmentation indices with a matrix of impact for application to all major global watersheds[4, 5]. Apart from time domain analyses, Discrete Fourier Transforms (DFTs) or wavelet analyses offer additional insights on impacts of flow alterations from human interventions[15, 20, 45, 57]. Consult Jumani et al.[38] for a review of river regulation and fragmentation indices including their applications, advantages and limitations.

While various approaches exist to infer hydrologic alterations from diversions, dam and reservoir operations including sub-daily hydropeaking cycles[58, 59], none focuses on the weekly timescale, a primary periodicity of socioeconomic activity. Therefore, we develop a novel WHI that combines time and frequency domain terms to quantify weekly

periodicity in river discharge. The time domain term (T_T, %) counts the number of weeks (D_w) in a given calendar year when two consecutive days exhibit flows lower than the corresponding weekly average ($\overline{Q_{1-7}}$), followed by five sequential days above the corresponding weekly average:

$$T_T = \max\left\{\frac{100}{52}\sum_{w=1}^{52} D_w\,, 0.001\right\} \text{ and where} \tag{1}$$

$$D_w = \left\{ \begin{array}{ll} 1 & \text{if } Q_{1,2} < \overline{Q_{1-7}} \text{ and if } Q_{3,\ldots,7} > \overline{Q_{1-7}} \\ 0.25 & \text{if } Q_1 < \overline{Q_{1-7}} \text{ and if } Q_{2,\ldots,7} > \overline{Q_{1-7}} \\ 0 & \text{if otherwise} \end{array} \right\}$$

This sequence of daily flows is chosen to emphasize the typical weekly rhythm observed in hydropeaking rivers: low flows on weekends when hydropower demand wanes, followed by high flows on weekdays when hydropower demand waxes[9]. A partial score of 0.25 is ascribed to sites where six consecutive days above the weekly average follow a single low flow day for that week. As some gauging sites lie downstream from points of regulation such that low flows are shifted later in the week rather than occurring on Saturdays and Sundays, we test all seven possible combinations of two consecutive days (e.g., Saturday/Sunday, Sunday/Monday, …, Friday/Saturday) and select the one that maximizes WHI at each site over the period of record. This approach for the time domain term attenuates the effects of cyclical (rather than periodic) variations from synoptic-scale storm activity, which otherwise leads to marked weekly cycles in pluvial rivers[45].

524 An application of DFTs to the daily discharge data provides the frequency domain term.
525 Here we follow Wilks[60] in partitioning the daily discharge time series into sine and
526 cosine waves of amplitude C_k for harmonic k. DFTs are computed for each calendar
527 year with the 52nd harmonic representing the weekly timescale of interest here. Then we
528 compute the explained variance of the 52nd harmonic (T_F):

529 $$T_F = \frac{\left(\frac{n}{2}\right)C_{52}^2}{(n-1)s_Q^2} \quad (2)$$

530

531 where n is the number of days in a given year (365 or 366 for a leap year), C_{52} is the
532 amplitude of the 52nd harmonic, and s_Q is the standard deviation in discharge.

533 After expressing T_T and T_F as percentages, we take the base 10 logarithm of their
534 product to obtain an annual WHI:

535 $$\text{WHI} = \log_{10}[B(T_T \times T_F)] \quad (3)$$

536 in which B (= 10) is a coefficient chosen so that the median WHI ≈ 0 among all 400
537 sites. Annual WHI values range typically from about -4 to +4 (although WHI values have
538 no theoretical upper or lower bounds), with large positive values indicating strong
539 weekly periodicity attributed to flow regulation at hydropower stations. In contrast, rivers
540 with robust annual cycles with flows dominated by potent snowmelt-driven freshets
541 and/or large (natural) storage capacity within abundant lakes, ponds and wetlands
542 exhibit large negative WHI values. The transition between negative to positive WHI
543 values marks a shift from annual to weekly dominant time scales of variability in flow.
544 The 1980-2019 mean daily flows (considering the day of the week) for the Stuart River
545 (BC), Mohawk River (New York), and Chattahoochee River at Buford Dam (Georgia)

illustrate the WHI ranging from the minimum, median, and maximum values (Supplementary Fig. 13). WHI values remain site-specific and must be interpreted with care, particularly moving away (both upstream and downstream) from measurement sites with an intervening body of water, a confluence or another point of regulation altering hydropeaking intensity.

Statistical analyses. We first compute WHI time series at all 400 sites and develop a 'climatology' of index values for 1980-2019, with 14 years ≤ n_y ≤ 40 years depending on data availability at each site. Summary statistics (mean, median, standard deviation, etc.) of the 1980-2019 WHI data are tabulated and their distribution tested for normality using the Shapiro-Wilk test. Similar climatological analyses are developed for each decade (1920s to 2010s) with results reported when n_y ≥ 5 years at a given site. The Mann-Kendall test (MKT[61, 62]) applied to all WHI time series with n_y ≥ 30 years over 1980-2019 yields linear, monotonic trends in hydropeaking intensity, with $p < 0.05$ considered locally statistically-significant. The field (or global) significance of the individual (or local) trend tests is assessed following Wilks[60]. The approach minimizes the false discovery rate (FDR) by first ranking *p*-values in ascending order for all trend tests with n_y ≥ 30 years. Trends are then globally significant if $p < p_{FDR}$ depending on the distribution of sorted *p*-values as:

$$p_{FDR} = \max_{i=1,2,\ldots,N} \{p_i : p_i \leq (i/N)\ \alpha_{\text{global}}\} \quad (4)$$

in which we set $\alpha_{\text{global}} = 0.10$. Trend analysis sensitivity to autocorrelation is tested in the Supplementary Methods.

We assess the 1920 to 2019 annual mean, median and maximum WHI across all sites with available data in a given year to track the overall evolution of hydropeaking intensity across the USA and Canada. We also count the annual number and percentage of sites that fall in the top decile of all 1920-2019 WHI scores. An additional metric reported is the discharge-weighted WHI_{Qj} computed each calendar year (index *j*) as:

$$\mathrm{WHI}_{\mathrm{Q_j}} = \sum_{i=1}^{n=400} \mathrm{WHI}_{i,j} \times \mathrm{Q}_{i,j} \,/\, \sum_{i=1}^{n=400} \mathrm{Q}_{i,j} \tag{5}$$

where $Q_{i,j}$ ($km^3\ yr^{-1}$) denotes the annual discharge and *i* is the site index. This yields a relative measure of annual volumetric flows affected by weekly hydropeaking cycles rather than just the number of sites. For monotonic trend analysis, the MKT is applied to time series of overall mean annual WHI over the 1980-2019 focus period. The potential influence of missing data on the evolution of average WHI over 1980-2019 is assessed by substituting incomplete time series with each missing site's average WHI computed over the remainder of the focus period. This yields an adjusted mean annual WHI time series for a first order assessment of the influence of incomplete data.

A histogram illustrates the distribution of two consecutive days when low flows emerge relative to the expected value of 1/7 = 0.143 were these randomly distributed. Fractions of the seven possible two-day combinations are partitioned according to WHI $\gtrless$ 0. The histogram also includes the corresponding mean WHI across all rivers for a given two-day combination of low flows. A Chi-Square goodness-of-fit test[63] verifies the hypothesis of whether the distribution of low flow days differs significantly from the expected value with threshold $p = 0.05$. Similarly, we test if the corresponding mean WHI values for the

two-day pairs with low flows follow a uniform distribution using a Chi-Square test. The relationship between annual WHI values and mean annual flows over 1980-2019 is evaluated using Pearson's correlation coefficient with $p < 0.05$ considered statistically-significant values. Next, we transform annual discharge time series to standardized anomalies over the period of record at each site (with < 10% missing data in a calendar year). Decadal mean standardized anomalies for all available sites are then computed when $n_y \geq 5$ years in a given decade. These decadal average anomalies are binned in increments of 0.25 standard anomaly for comparison with WHI decadal distributions.

To explore possible factors contributing to WHI trends we assess whether the dispersion of flows across the seven days of the week is changing over time. Here we first compile total annual flows (in $m^3 s^{-1}$) for each of the seven days of the week, as well as the overall average, over each calendar year. Then we quantify departures (as a percentage) for each day of the week relative to the annual mean. Next, we calculate standard deviations (σ) in the percentage departures for the seven days of the week each year, creating σ time series for all 400 sites over 1980-2019. Finally, application of the MKT on the σ time series (when $n_y \geq 30$ years) yields 1980-2019 dispersion trends.

Data availability

Data related to this article can be found in the Supplementary Information and Supplementary Data files. Discharge data used in this study are available in the following publicly accessible databases: Centre d'Expertise Hydrique du Québec (http://www.cehq.gouv.qc.ca/hydrometrie/historique_donnees/info_validite.htm), US Bureau of Reclamation (https://data.usbr.gov/), United States Geological Survey

(https://waterdata.usgs.gov/nwis), Water Survey of Canada's Hydrometric Database (https://wateroffice.ec.gc.ca), Idaho Power (https://idastream.idahopower.com/Data/) and the International Boundary and Water Commission (https://www.ibwc.gov/Water_Data/). For some regulated rivers, proprietary discharge data can be requested from the following data providers: BC Hydro, Evolugen, H2O Power, Hydro-Québec, International Boundary and Water Commission, Manitoba Hydro, Nalcor Energy, NB Power, Ontario Power Generation, Rio Tinto, Tennessee Valley Authority, and TransAlta (see Supplementary Table 3). Source data are provided with this paper.

Code availability

The Fortran code used in this study is available online with explanation at http://web.unbc.ca/~sdery/NatComm.zip.

References

1. International Hydropower Association. 2020 Hydropower Status Report, https://hydropower-assets.s3.eu-west-2.amazonaws.com/publications-docs/2020_hydropower_status_report.pdf (2020).
2. Graf, W. L. Dam nation: A geographic census of American dams and their large-scale hydrologic impacts. *Water Resour. Res.* **35**, 1305-1311 (1999).
3. Couto, T. B. A. & Olden, J. D. Global proliferation of small hydropower plants: science and policy. *Front. Ecol. Environ.* **16**, 91-100 (2018).
4. Dynesius, M. & Nilsson, C. Fragmentation and flow regulation of river systems in the northern third of the world. *Science* **266**, 753-762 (1994).
5. Grill, G. et al. An index-based framework for assessing patterns and trends in river fragmentation and flow regulation by global dams at multiple scales. *Environ. Res. Lett.* **10**, 015001 (2015).
6. Grill, G. et al. Mapping the world's free-flowing rivers. *Nature* **569**, 215-219 (2019).

7. Mideksa, T. K. & Kallbekken, S. The impact of climate change on the electricity markets: A review. *Energ. Policy* **38**, 3579-3585 (2010).

8. Wang, C., Grozev, G. & Seo S. Decomposition and statistical analysis for regional electricity demand forecasting. *Energy* **41**, 313-325 (2012).

9. Rosenberg, D. M. et al. Large-scale impacts of hydroelectric development. *Environ. Rev.* **5**, 27-54 (1997).

10. Contosta, A. R., Casson, N. J., Nelson, S. J. & Garlick, S. Defining frigid winter illuminates its loss across seasonally snow-covered areas of eastern North America. *Environ. Res. Lett*. **15**, 034020 (2020).

11. Perkins-Kirkpatrick, S. E. & Lewis, S. C. Increasing trends in regional heat waves. *Nat. Comm.* **11**, 3357 (2020).

12. Barthendu, S. & Cohen, S. J. Impact of CO2-induced climate change on residential heating and cooling energy requirements in Ontario, Canada. *Energ. Buildings* **10**, 99-108 (1987).

13. Filion, Y. Climate change: Implications for Canadian water resources and hydropower production. *Can. Water Resour. J.* **25**, 255-269 (2000).

14. Schaeffer, R. et al. Energy sector vulnerability to climate change: A review. *Energy* **38**, 1-12 (2012).

15. Déry, S. J., Stadnyk, T. A., MacDonald, M. K., Koenig, K. A. & Guay, C. Flow alteration impacts on Hudson Bay river discharge. *Hydrol. Process.* **32**, 3576-3587 (2018).

16. Greimel, F. et al. Chapter 5: Hydropeaking Impacts and Mitigation. In: Schmutz S., Sendzimir J. (eds) Riverine Ecosystem Management. Aquatic Ecology Series, vol 8. Springer, Cham, https://doi.org/10.1007/978-3-319-73250-3_5 (2018).

17. Smokorowski, K. E. The ups and downs of hydropeaking: a Canadian perspective on the need for, and ecological costs of, peaking hydropower production. *Hydrobiologia* doi: 10.1007/s10750-020-04480-y (2021).

18. Battala, R. J. et al. Hydropeaked rivers need attention. *Environ. Res. Lett*. **16**, 021001 (2021).

19. She, Y., Hicks, F. & Andrishak, R. The role of hydro-peaking in freeze-up consolidation events on regulated rivers. *Cold Reg. Sci. Technol.* **73**, 41-49 (2012).

20. White, M. A., Schmidt, J. C. & Topping, D. J. Application of wavelet analysis for monitoring the hydrologic effects of dam operation: Glen Canyon Dam and the Colorado River at Lees Ferry, Arizona. *River Res. Appl.* **21**, 551-565 (2005).

21. Horner, N. C., Shehabi, A. & Azevedo, I. Known unknowns: Indirect energy effects of information and communication technology. *Environ. Res. Lett.* **11**, 103001 (2016).

22. Skuterud, M. The impact of Sunday shopping on employment and hours of work in the retail industry: Evidence from Canada. *European Economic Rev.* **49**, 1953-1978 (2005).

23. Anderson, E. P. et al. Understanding rivers and their social relations: a critical step to advance environmental water management. *Wiley Interdisciplinary Reviews: Water* **6**, p.e1381 (2019).

24. Auer, N. A. Response of spawning lake sturgeons to change in hydroelectric facility operation. *T. Am. Fish. Soc.* **125**, 66-77 (1996).

25. Karier, T. Economics of the Columbia River Treaty. *Electr. J.* **33**, 106731 (2020).

26. Matbouli, Y. T., Hipel, K. W. & Kilgour, D. M. Strategic analysis of the Great Canadian hydroelectric power conflict. *Energy Strateg. Rev.* **4**, 43-51 (2014).

27. Hydro-Québec. Hydro-Québec: North America's leading provider of clean energy, https://www.hydroquebec.com/clean-energy-provider/, (2020).

28. Voisin, N. et al. Impact of climate change on water availability and its propagation through the western U.S. power grid. *Appl. Energy* **276**, 115467 (2020).

29. Bejarano, M. D., Jansson, R. & Nilsson, C. The effects of hydropeaking on riverine plants: a review. *Biol. Rev.* **93**, 658-673 (2018).

30. Moreira, M. et al. Ecologically-based criteria for hydropeaking mitigation: A review. *Sci. Total Environ.* **657**, 1508-1522 (2019).

31. Serreze, M. C. & Francis, J. A. The Arctic amplification debate. *Clim. Change* **76**, 241–265 (2006).

32. Poff, N. L. & Schmidt, J. C. How dams can go with the flow. *Science* **353**, 1099-1100 (2016).

33. Harvey-Lavoie, S., Cooke, S. J., Guénard, G. & Boisclair, D. Differences in movements of northern pike inhabiting rivers with contrasting flow regimes, *Ecohydrology* **9**, 1687-1699 (2016).

34. Jones, N. E. & Petreman, I. C. Environmental influences on fish migration in a hydropeaking river. *River Res. Appl.* **31**, 1109-1118 (2015).

35. Kelly, B., Smokorowski, K. E. E. & Power, M. Downstream effects of hydroelectric dam operation on thermal habitat use by Brook Trout (*Salvelinus fontinalis)* and Slimy Sculpin (*Cottus cognatus*). *Ecol. Freshw. Fish* **26**, 552-562 (2017).

36. Taylor, M. K. et al. Reach-scale movements of bull trout (*Salvelinus confluentus*) relative to hydropeaking operations in the Columbia River, Canada. *Ecohydrology* **7**, 1079-1086 (2014).

37. Haghighi, A. T., Marttila, H. & Klove, B. Development of a new index to assess river regime impacts after dam construction. *Global Planet. Change* **122**, 186-196 (2014).

38. Jumani, S. et al. River fragmentation and flow alteration metrics: a review of methods and directions for future research. *Environ. Res. Lett.* **15**, 123009 (2020).

39. Mlynowski, T. J., Hernández-Henríquez, M. A. & Déry, S. J. An evaluation of hydrometric monitoring across the Canadian pan-Arctic region, 1950-2008. *Hydrol. Res.* **42**, 479-490 (2011).

40. Gleason, C. J. & Smith, L. C. Toward global mapping of river discharge using satellite images and at-many-stations hydraulic geometry. *Proc. Natl Acad. Sci. USA* **111**, 4788-4791 (2014).

41. Tongal, H. & Booij, M. J. Simulation and forecasting of streamflows using machine learning models coupled with base flow separation. *J. Hydrol.* **564**, 266-282 (2018).

42. Tefs, A. A. G. et al. Simulating river regulation and reservoir performance in a continental-scale hydrologic model. *Environ. Modell. Softw.*, in press (2021).

43. Benke, A. C. & Cushing, C. E. (Eds.) *Rivers of North America*. Elsevier Academic Press, Amsterdam, 1144 pp. (2005).

44. Déry, S. J. et al. Detection of runoff timing changes in pluvial, nival and glacial rivers of western Canada. *Water Resour. Res.* **45**, W04426 (2009).

45. Smith, L. C., Turcotte, D. L. & Isacks, B. L. Stream flow characterization and feature detection using a discrete wavelet transform. *Hydrol. Process.* **12**, 233-249 (1998).

46. Déry, S. J., Stadnyk, T. A., MacDonald, M. K. & Gauli-Sharma, B. Recent trends and variability in river discharge across northern Canada. *Hydrol. Earth Syst. Sci.* **20**, 4801-4818 (2016).

47. Déry, S. J., Stieglitz, M., McKenna, E. C. & Wood, E. F. Characteristics and trends of river discharge into Hudson, James, and Ungava Bays, 1964–2000. *J. Clim.* **18**, 2540–2557 (2005).

48. Peters, D. L. & Buttle, J. M. The effects of flow regulation and climatic variability on obstructed drainage and reverse flow contribution in a northern river-lake-delta complex, Mackenzie Basin headwaters. *River Res. Appl.* **26**, 1065-1089 (2010).

49. Woo, M., Thorne, R., Szeto, K. & Yang, D. Streamflow hydrology in the boreal region under the influence of climate and human interference. *Philos. T. R. Soc. B.* **363**, 2251-2260 (2008).

50. Assani, A. A., Stichelbout, E., Roy, A. G. & Petit, F. Comparison of impacts of dams on the annual maximum flow characteristics in three regulated hydrologic regimes in Québec (Canada). *Hydrol. Process.* **20**, 3485-3501 (2006).

51. Naik, P. K. & Jay, D. A. Distinguishing human and climate influences on the Columbia River: Changes in mean flow and sediment transport. *J. Hydrol.* **404**, 259-277 (2011).

52. St. Jacques, J.-M., Sauchyn, D. J. & Zhao, Y. Northern Rocky Mountain streamflow records: Global warming trends, human impacts or natural variability? *Geophys. Res. Lett.* **37**, L06407 (2010).

53. Ye, B., Yang, D. & Kane, D. L. Changes in Lena River streamflow hydrology: Human impacts versus natural variations. *Water Resour. Res.* **39**, 1200 (2003).

54. Richter, B. D., Baumgartner, J. V., Powell, J. & Braun, D. P. A method for assessing hydrologic alteration within ecosystems. *Conserv. Biol.* **10**, 1163-1174 (1996).

55. Timpe, K. & Kaplan, D. The changing hydrology of a dammed Amazon. *Sci. Adv.* **3**, e1700611 (2017).

56. Zhou, X., Huang, X., Zhao, H. & Ma, K. Development of a revised method for indicators of hydrologic alteration for analyzing the cumulative impacts of cascading reservoirs on flow regime. *Hydrol. Earth Syst. Sci.* **24**, 4091-4107 (2020).

57. Tongal, H., Demirel, M. C. & Moradkhani, H. Analysis of dam-induced patterns on river flow dynamics. *Hydrol. Sci. J.* **62**, 626-641 (2017).

58. Carolli, M. et al. A simple procedure for the assessment of hydropeaking flow alterations applied to several European streams. *Aquat. Sci.* **77**, 639-653 (2015).

59. Ashraf, F. B. H. et al. Changes in short term river flow regulation and hydropeaking in Nordic rivers. *Sci. Rep.* **8**, 17232 (2018).

60. Wilks, D. S. *Statistical Methods in the Atmospheric Sciences*, Elsevier, Amsterdam, 4th edition, 818 pp. (2019).

61. Mann, H. B. Non-parametric test against trend. *Econometrika* **13**, 245–259 (1945).

62. Kendall, M. G. *Rank Correlation Methods*. 202 pp., Oxford Univ. Press, New York (1975).

63. McCuen, R. H. *Modeling Hydrologic Change: Statistical Methods*. Lewis Publishers, Boca Raton, 433 pp. (2003).

Acknowledgements. Thanks to the Water Survey of Canada and its provincial and territorial partners, the Centre d'Expertise Hydrique du Québec, USGS, BC Hydro, Evolugen by Brookfield Renewable, Transalta, Manitoba Hydro, Ontario Power Generation, H2O Power, Rio Tinto, Hydro-Québec, NB Power, Nalcor Energy, Idaho Power, the Tennessee Valley Authority, the International Boundary and Water Commission and the US Bureau of Reclamation for providing hydrometric data. Thanks to Aseem Sharma (UNBC/NRCan) for preparing the spatial plots, Clyde McLean and Joanna Barnard (Nalcor Energy), Jim Samms (NB Power), Marie Broesky, Kevin Gawne, Kristina Koenig, Phil Slota, Kevin Sydor, Efrem Teklemariam, Mike Vieira and Shane Wruth (Manitoba Hydro), Matt MacDonald (Ontario Power Generation), Erik Richards and Marc Mantha (H2O Power), Samer Alghabra and Mokhtar Moujahid (Hydro-Québec), Bruno Larouche and Richard Loubier (Rio Tinto), Michael Smilski (Transalta), Jim Li, Debbie Rinvold and Stephanie Smith (BC Hydro), Adrian Cortez and

Delbert Humberson (International Boundary and Water Commission), Kelly Withers and Matti Hanninen (Evolugen) for providing comments on this work and for additional data for regulated rivers, Dwayne Akerman, Amber Brown, Michel Desjardins, Matt Falcone, Samantha Hussey, Lyssa Maurer, Angus Pippy, Melanie Taylor, and Frank Weber (Water Survey of Canada) for sharing supplemental hydrometric data, and Huilin Gao (Texas A&M), John Zhu (Texas Water Development Board), Julie Thériault (UQAM) and Mike Vieira and Kristina Koenig (Manitoba Hydro) for logistical support. This research was supported by the Natural Sciences and Engineering Research Council of Canada, Manitoba Hydro, and partners through funding of the BaySys project.

Author contributions. S.J.D. designed the study, extracted hydrometric data and constructed time series of daily discharge for all rivers, formulated the weekly hydropeaking index, developed the codes, performed the statistical and computational analyses, and drafted line graphs with support from M.A.H.H., T.A.S., and T.J.T. S.J.D. wrote the manuscript with contributions from all co-authors and all contributed to manuscript refinement and revisions.

Competing interests. The authors declare no competing interests.

Figure Legends

Fig. 1 Map of the 1980-2019 mean WHI values for 400 sites across the USA and Canada. Circle size corresponds to the two consecutive days with low flows beginning with the Saturday/Sunday (SS, largest symbols) combination and ending with the Friday/Saturday (FS, smallest symbols).

Fig. 2 Histogram of the 1980-2019 frequency distribution of low flow days and corresponding WHI values. Black bars denote the two consecutive days with low flows while red bars represent the WHI values for 400 sites across the USA and Canada, 1980-2019. Fractions of the two consecutive days with low flows are partitioned according to positive (solid) and negative (hatched) WHI values. The days of the week begin with the Saturday/Sunday (SS) combination and end with the Friday/Saturday (FS) combination. The horizontal black line denotes the expected value if the two-day low flows were distributed randomly while the horizontal red line marks the mean WHI across the 400 sites.

Fig. 3 Maps of the decadal mean WHI values for 400 sites across the USA and Canada. Maps are shown for **a** 1920-1929, **b** 1930-1939, **c** 1940-1949, **d** 1950-1959, **e** 1960-1969, **f** 1970-1979, **g** 1980-1989, **h** 1990-1999, **i** 2000-2009, and **j** 2010-2019. Circle size corresponds to the two consecutive days with low flows beginning with the Saturday/Sunday (SS, largest symbols) combination and ending with the Friday/Saturday (FS, smallest symbols). Results are shown only when $n_y \geq 5$ years in a given decade. Panels **k** and **l** represent the cumulative percentage of sites falling within one of 10 WHI bins and one of seven two-day combinations of low flows, respectively. In **k**, WHI bins match those used in the spatial plots **a-j** with a similar color palette (e.g., the maroon bars indicate WHI ≥ 3.0 starting at a zero cumulative percentage). In **l**, the two-day combinations with low flows start on Friday/Saturday at a zero cumulative percentage (maroon bars) and end on Saturday/Sunday at 100% (black bars).

Fig. 4 Map of the 1980-2019 monotonic trends in WHI at 380 sites across the USA and Canada. Red upward (blue downward) pointing triangles indicate positive (negative) trends. Trend magnitudes are proportional to the triangle sizes and green circles (pink outlines) indicate locally (globally) statistically-significant trends ($p < 0.05$). Results are shown only when $n_y \geq 30$ years.

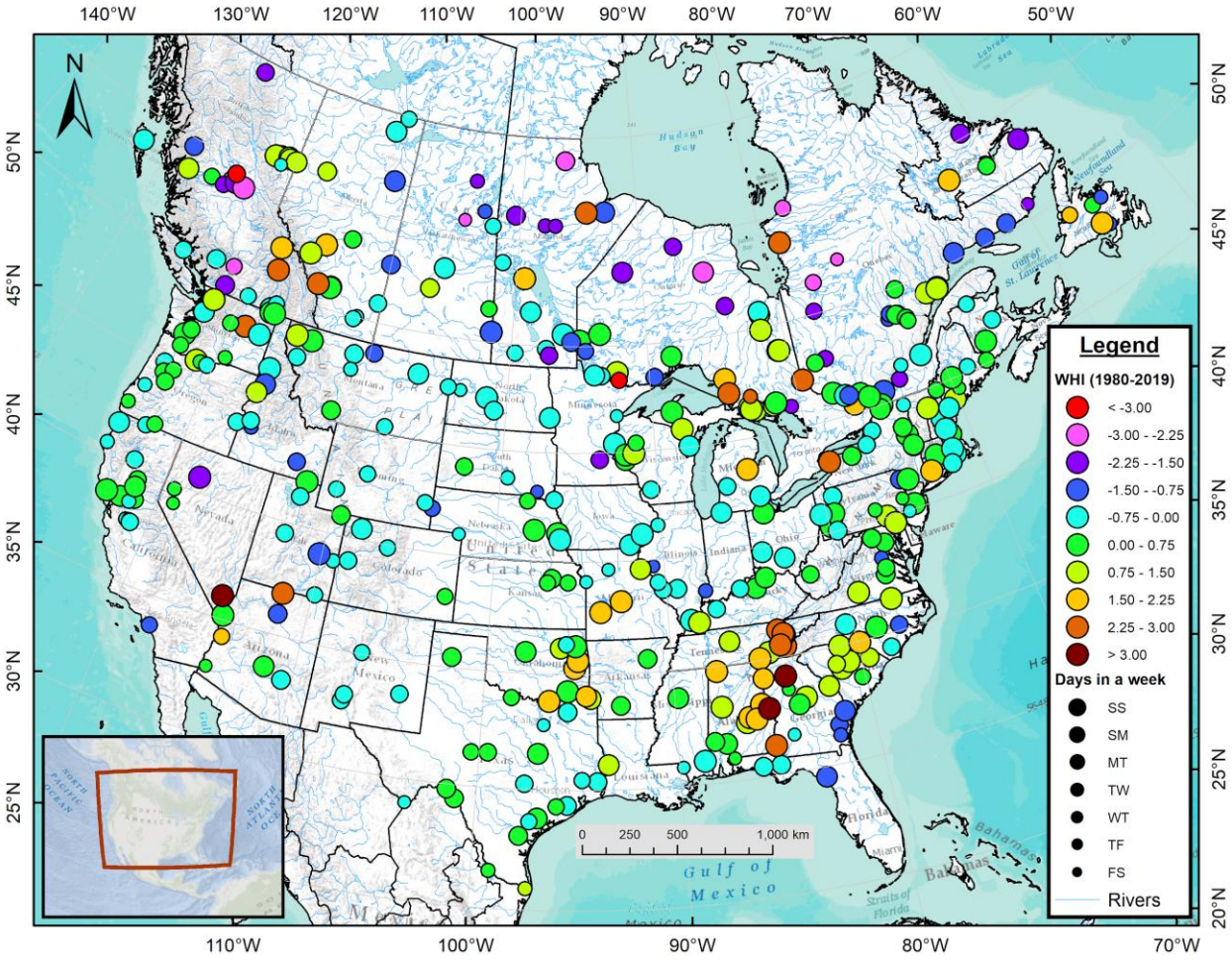

Fig. 1 Map of the 1980-2019 mean WHI values for 400 sites across the USA and Canada. Circle size corresponds to the two consecutive days with low flows beginning with the Saturday/Sunday (SS, largest symbols) combination and ending with the Friday/Saturday (FS, smallest symbols).

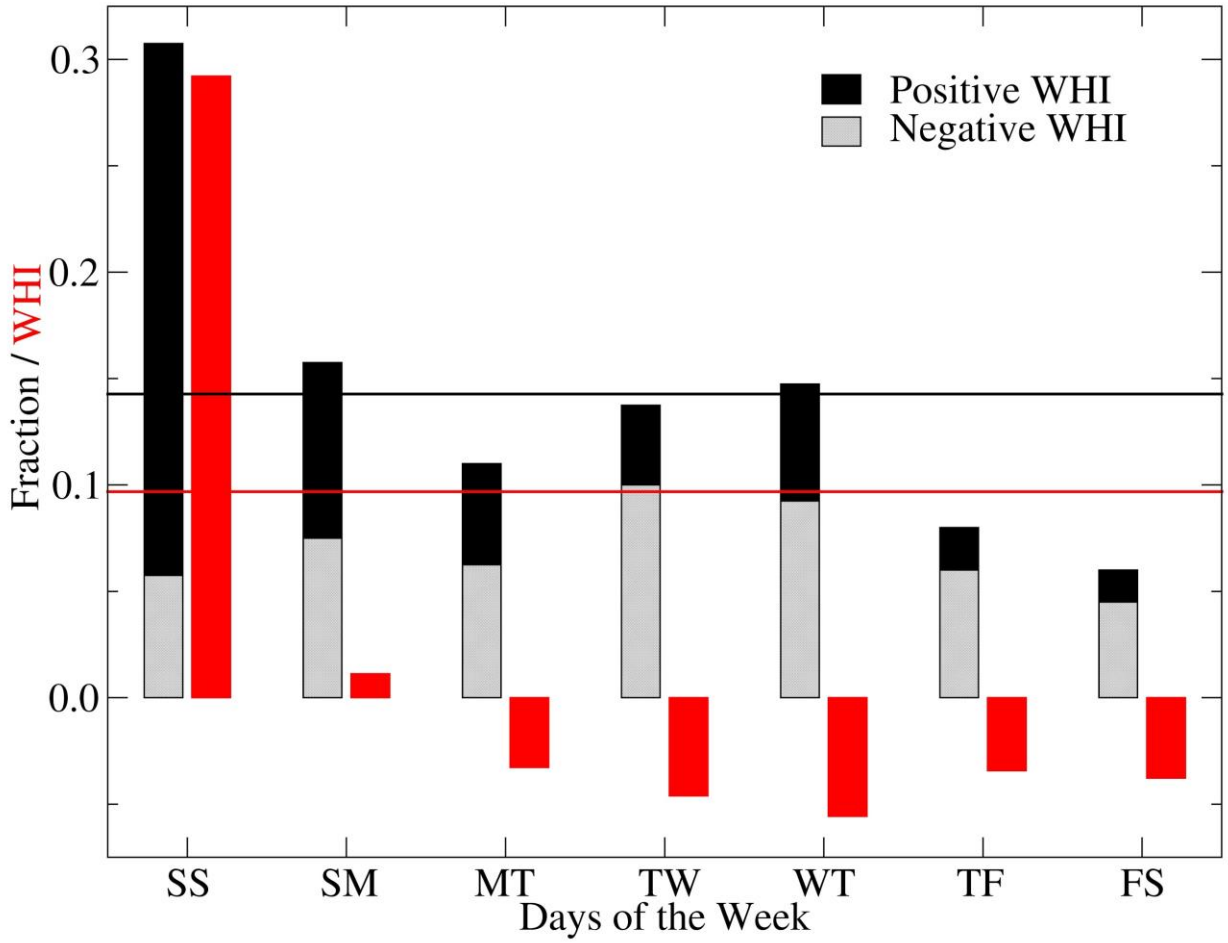

Fig. 2 Histogram of the 1980-2019 frequency distribution of low flow days and corresponding WHI values. Black bars denote the two consecutive days with low flows while red bars represent the WHI values for 400 sites across the USA and Canada, 1980-2019. Fractions of the two consecutive days with low flows are partitioned according to positive (solid) and negative (hatched) WHI values. The days of the week begin with the Saturday/Sunday (SS) combination and end with the Friday/Saturday (FS) combination. The horizontal black line denotes the expected value if the two-day low flows were distributed randomly while the horizontal red line marks the mean WHI across the 400 sites.

885 **a 1920-1929**

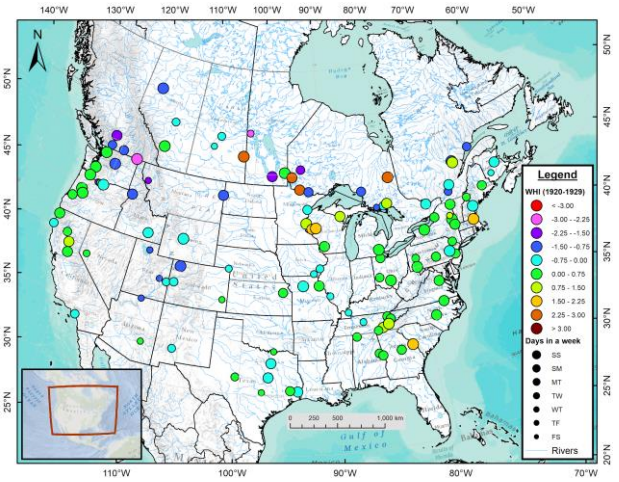

b 1930-1939

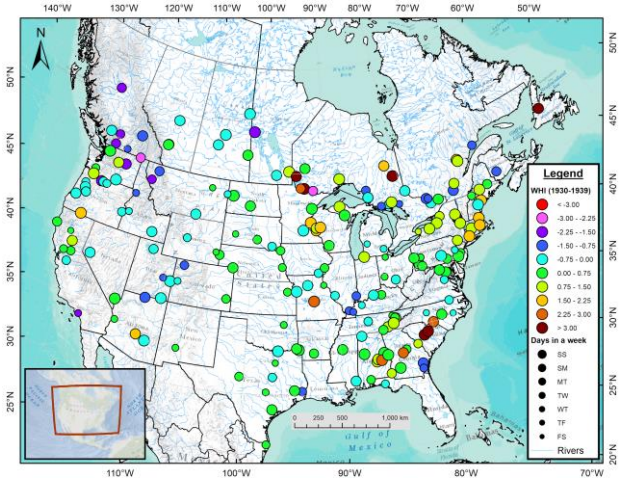

886

887 **c 1940-1949**

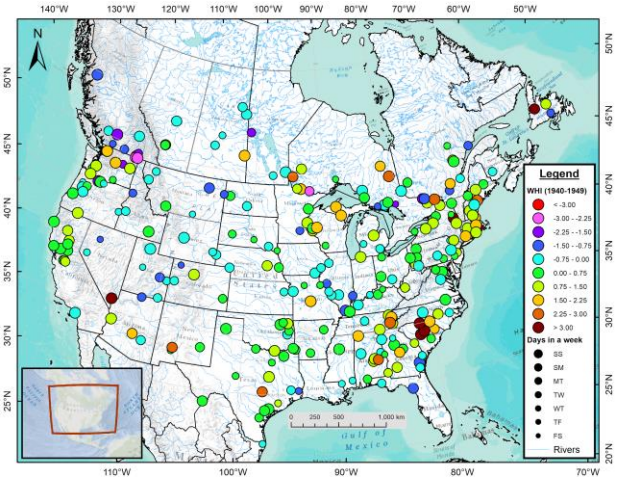

d 1950-1959

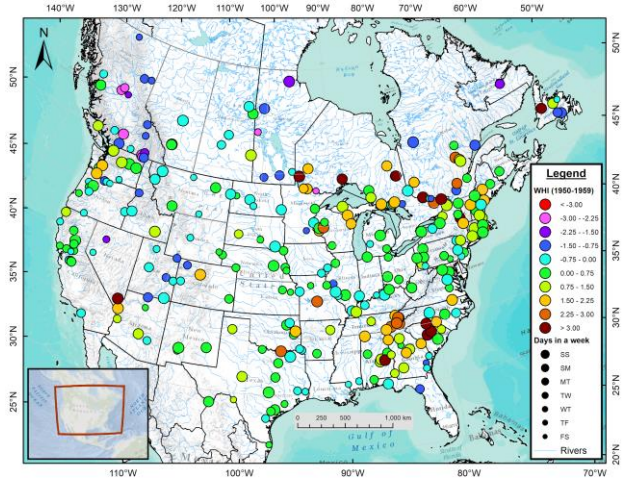

888

889 **e 1960-1969**

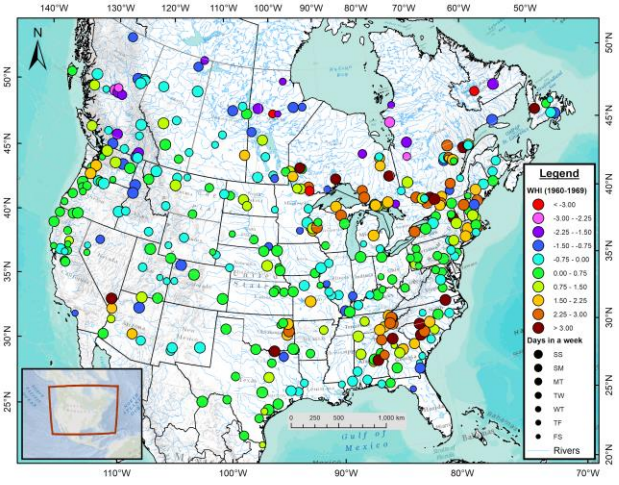

f 1970-1979

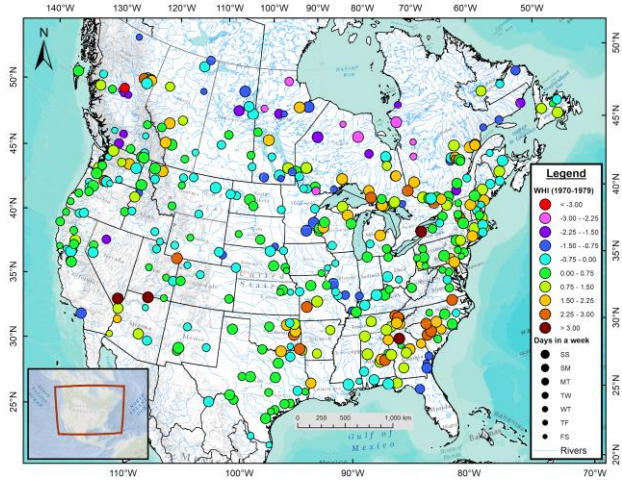

890

891 **g 1980-1989** **h 1990-1999**

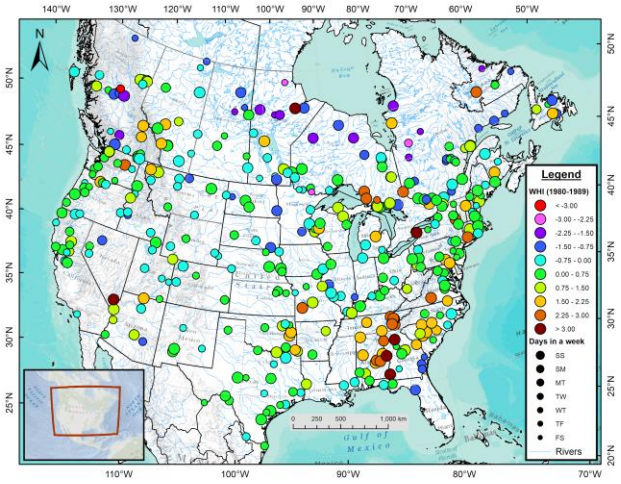

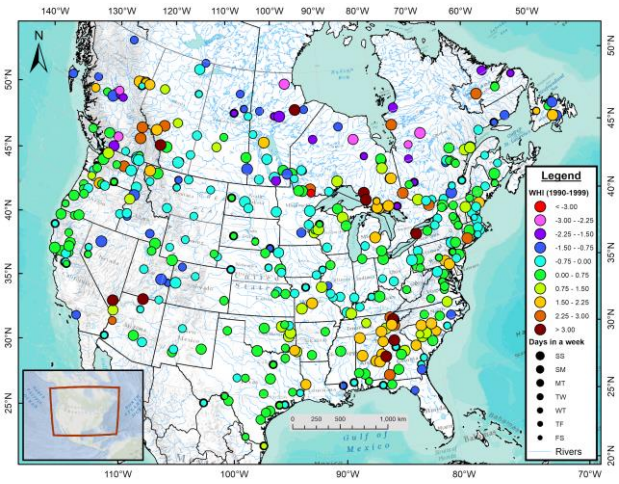

892

893 **i 2000-2009** **j 2010-2019**

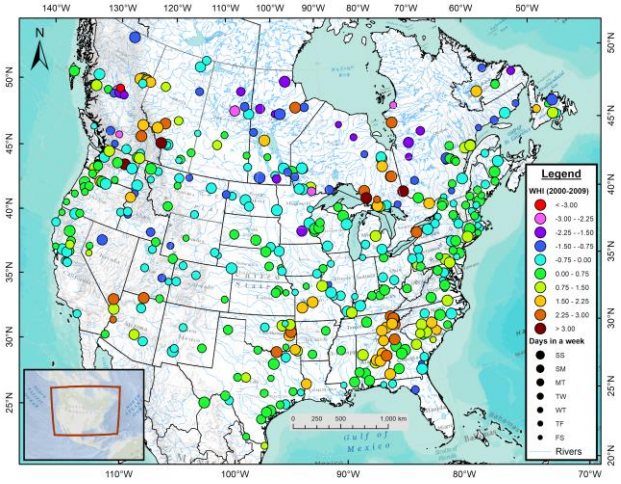

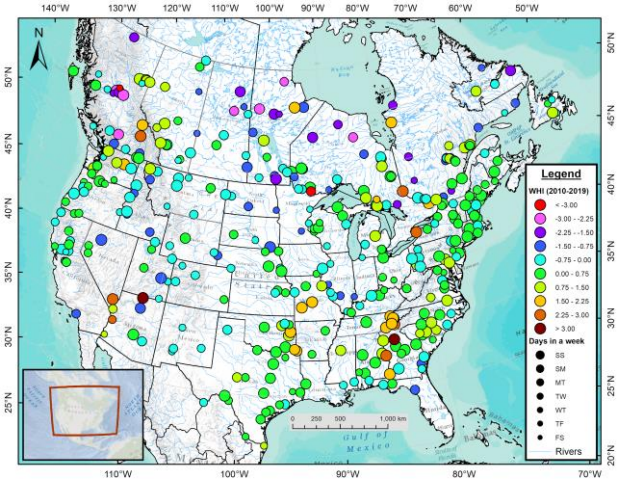

894

895 **k** **l**

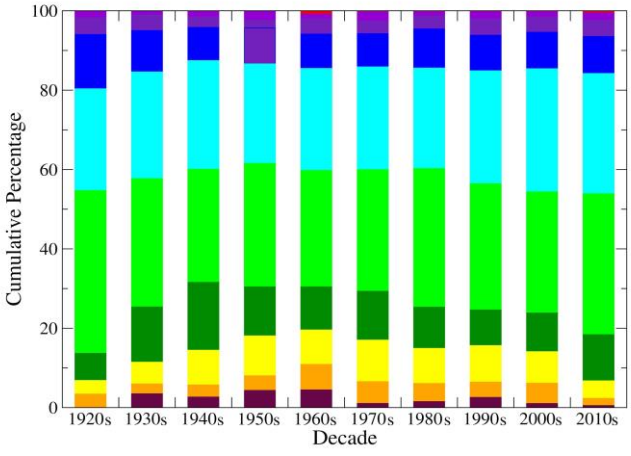

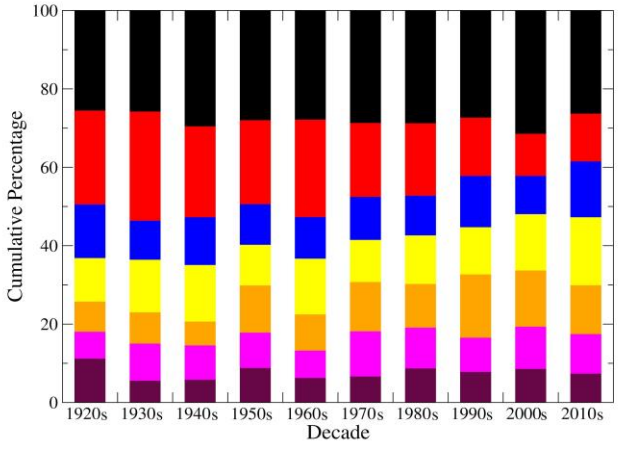

Fig. 3 Maps of the decadal mean WHI values for 400 sites across the USA and Canada. Maps are shown for **a** 1920-1929, **b** 1930-1939, **c** 1940-1949, **d** 1950-1959, **e** 1960-1969, **f** 1970-1979, **g** 1980-1989, **h** 1990-1999, **i** 2000-2009, and **j** 2010-2019. Circle size corresponds to the two consecutive days with low flows beginning with the Saturday/Sunday (SS, largest symbols) combination and ending with the Friday/Saturday (FS, smallest symbols). Results are shown only when $n_y \geq 5$ years in a given decade. Panels **k** and **l** represent the cumulative percentage of sites falling within one of 10 WHI bins and one of seven two-day combinations of low flows, respectively. In **k**, WHI bins match those used in the spatial plots **a-j** with a similar color palette (e.g., the maroon bars indicate WHI ≥ 3.0 starting at a zero cumulative percentage). In **l**, the two-day combinations with low flows start on Friday/Saturday at a zero cumulative percentage (maroon bars) and end on Saturday/Sunday at 100% (black bars).

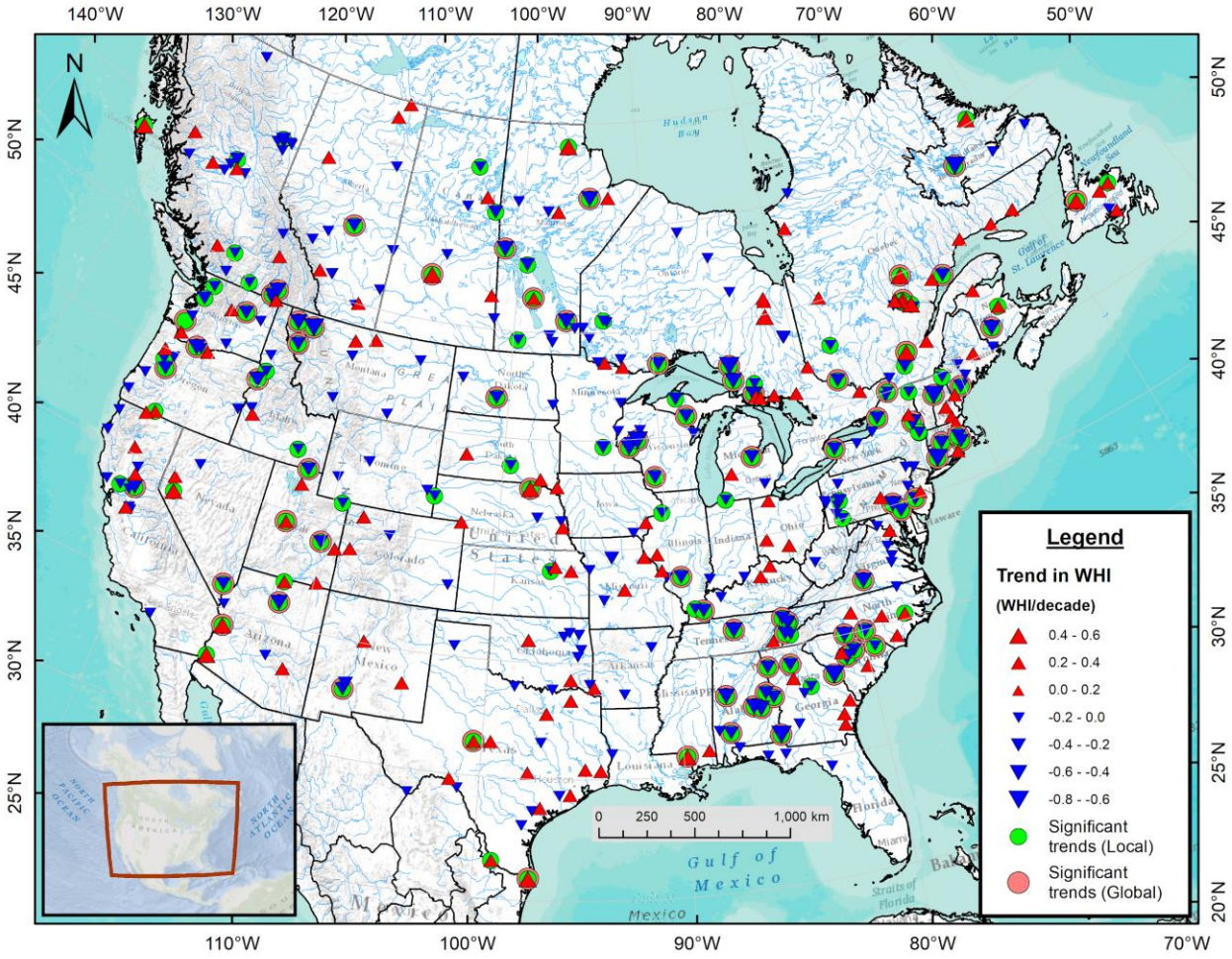

Fig. 4 Map of the 1980-2019 monotonic trends in WHI at 380 sites across the USA and Canada. Red upward (blue downward) pointing triangles indicate positive (negative) trends. Trend magnitudes are proportional to the triangle sizes and green circles (pink outlines) indicate locally (globally) statistically-significant trends ($p < 0.05$). Results are shown only when $n_y \geq 30$ years.

Table 1 List of sites with the top ten ranking WHI values, 1980-2019.

Rank	Site	WHI
1	Chattahoochee R. at Buford Dam (GA)	3.299
2	Chattahoochee R. at West Point (GA)	3.276
3	Colorado R. at Hoover Dam (AZ/NV)	3.222
4	Nelson R. (MB)	2.916
5	Niagara R. (ON/NY)	2.900
6	Colorado R. at Lees Ferry (AZ)	2.844
7	Montreal R. (Lake Superior, ON)	2.790
8	Montreal R. (Ottawa Basin, ON)	2.716
9	Holston R. at Cherokee Dam (TN)	2.675
10	Columbia R. at Grand Coulee Dam (WA)	2.662

AZ: Arizona, GA: Georgia, MB: Manitoba, NV: Nevada, NY: New York, ON: Ontario, TN: Tennessee, WA: Washington

Figures

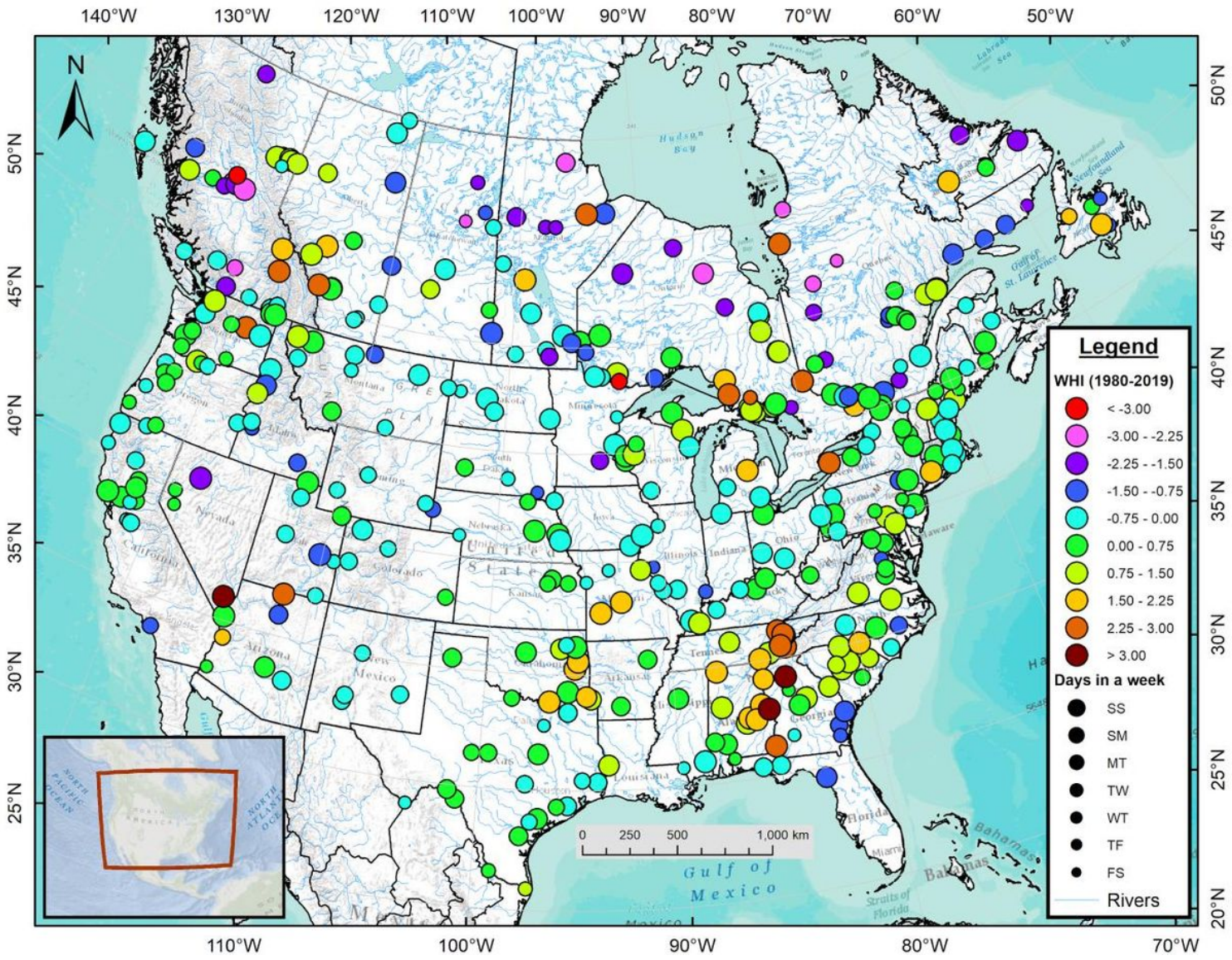

Figure 1

Map of the 1980-2019 mean WHI values for 400 sites across the USA and Canada. Circle size corresponds to the two consecutive days with low flows beginning with the Saturday/Sunday (SS, largest symbols) combination and ending with the Friday/Saturday (FS, smallest symbols).

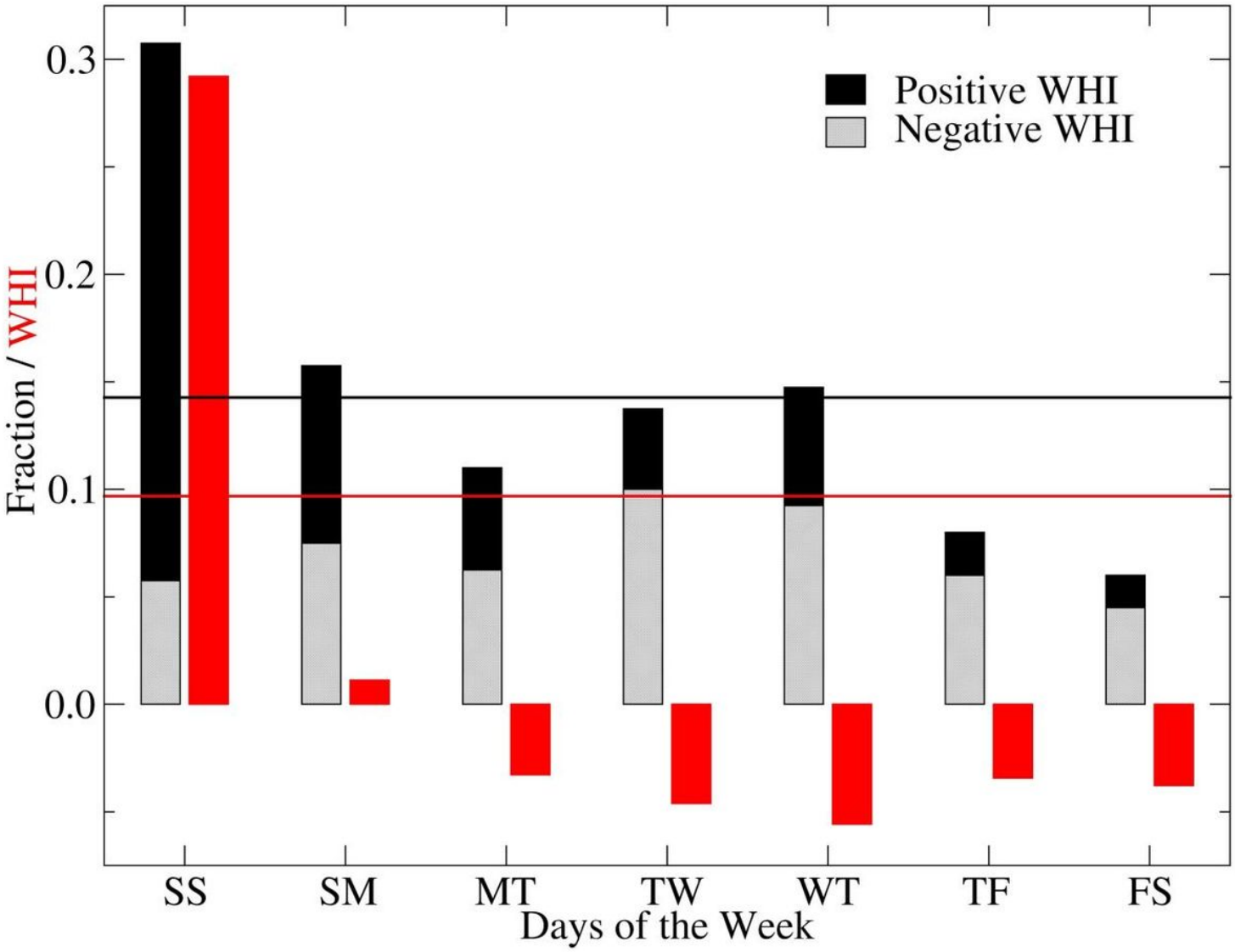

Figure 2

Histogram of the 1980-2019 frequency distribution of low flow days and corresponding WHI values. Black bars denote the two consecutive days with low flows while red bars represent the WHI values for 400 sites across the USA and Canada, 1980-2019. Fractions of the two consecutive days with low flows are partitioned according to positive (solid) and negative (hatched) WHI values. The days of the week begin with the Saturday/Sunday (SS) combination and end with the Friday/Saturday (FS) combination. The horizontal black line denotes the expected value if the two-day low flows were distributed randomly while the horizontal red line marks the mean WHI across the 400 sites.

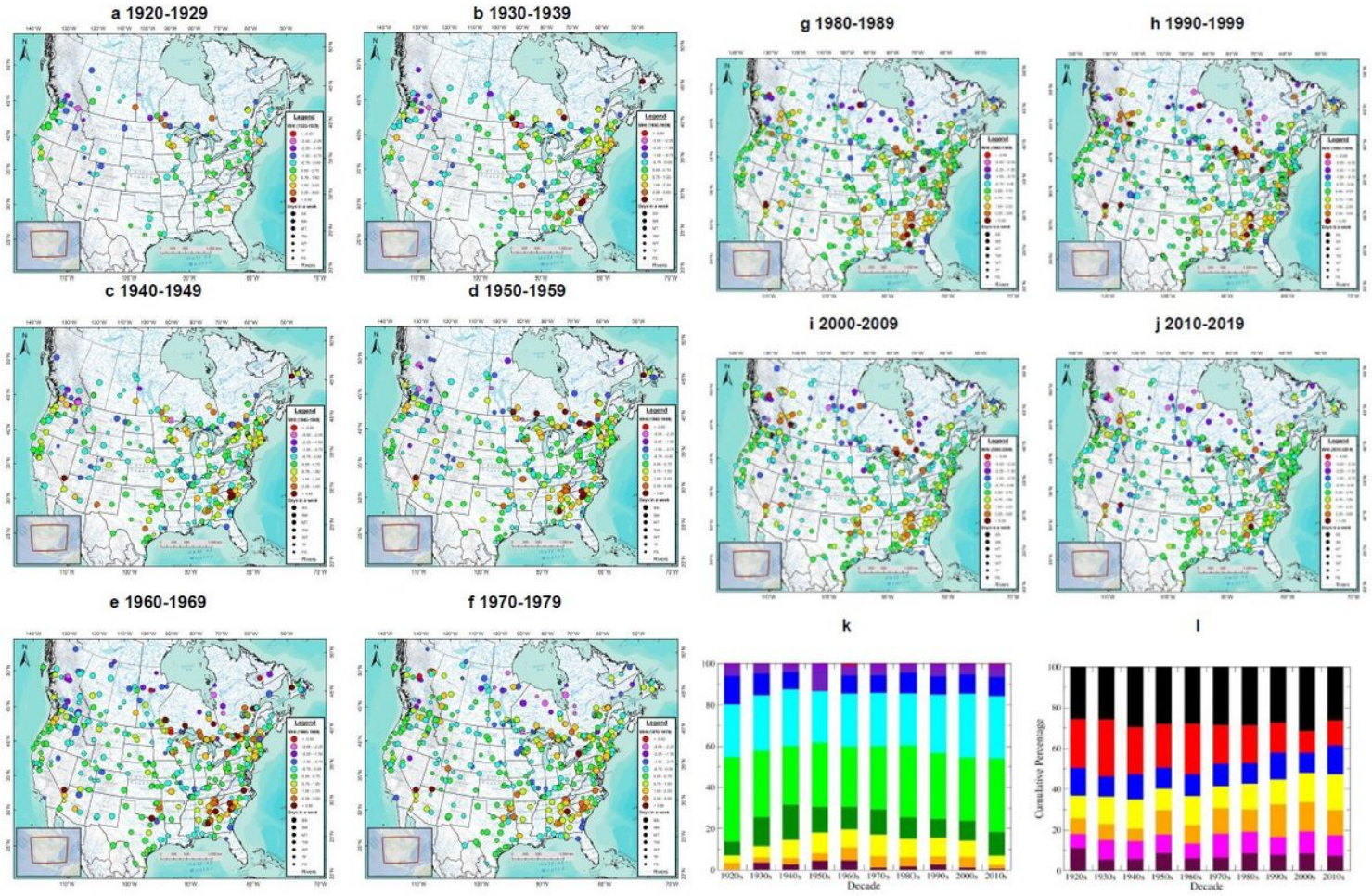

Figure 3

Maps of the decadal mean WHI values for 400 sites across the USA and Canada. Maps are shown for a 1920-1929, b 1930-1939, c 1940-1949, d 1950-1959, e 1960-1969, f 1970-1979, g 1980-1989, h 1990-1999, i 2000-2009, and j 2010-2019. Circle size corresponds to the two consecutive days with low flows beginning with the Saturday/Sunday (SS, largest symbols) combination and ending with the Friday/Saturday (FS, smallest symbols). Results are shown only when ny ≥ 5 years in a given decade. Panels k and l represent the cumulative percentage of sites falling within one of 10 WHI bins and one of seven two-day combinations of low flows, respectively. In k, WHI bins match those used in the spatial plots a-j with a similar color palette (e.g., the maroon bars indicate WHI ≥ 3.0 starting at a zero cumulative percentage). In l, the two-day combinations with low flows start on Friday/Saturday at a zero cumulative percentage (maroon bars) and end on Saturday/Sunday at 100% (black bars).

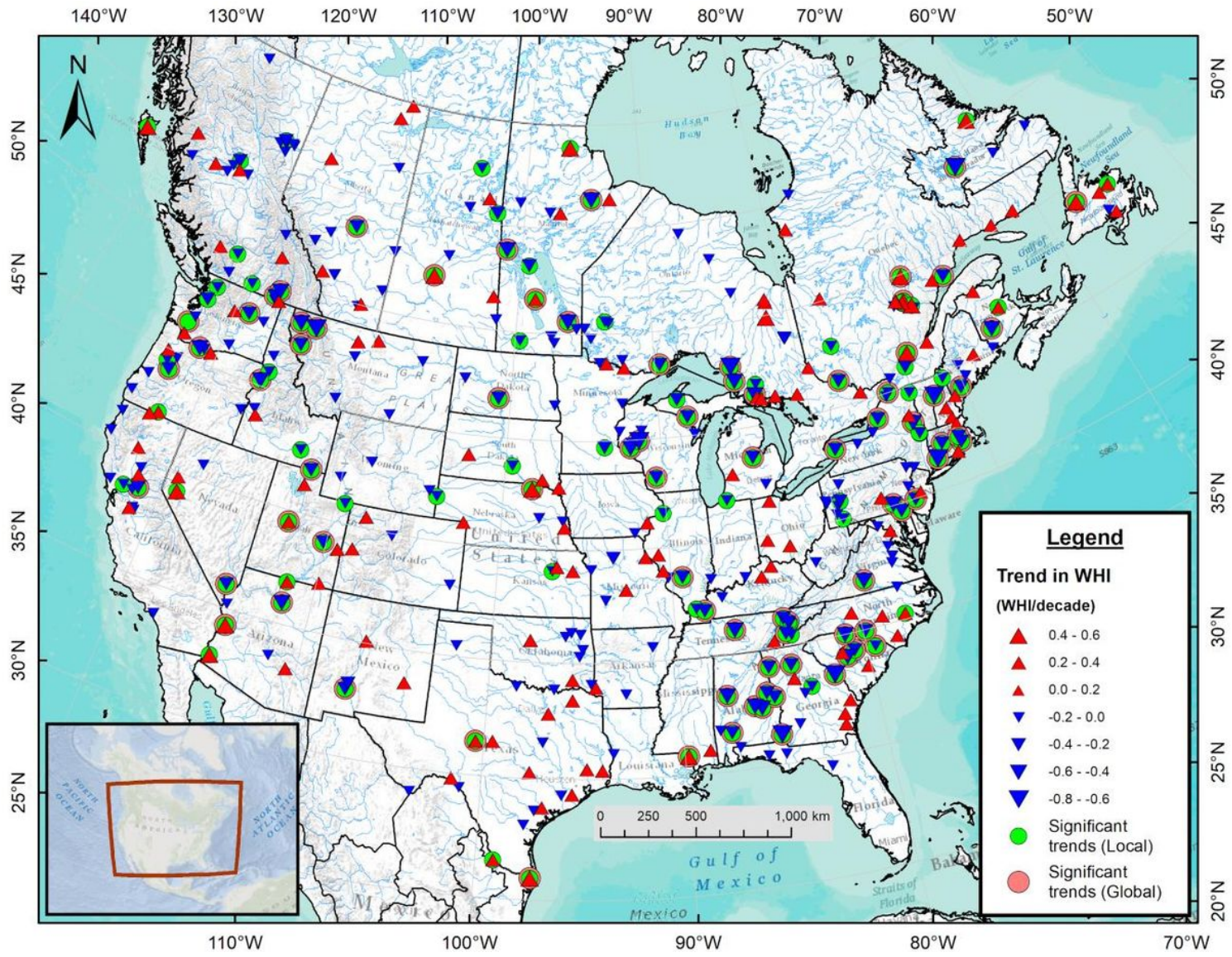

Figure 4

Map of the 1980-2019 monotonic trends in WHI at 380 sites across the USA and Canada. Red upward (blue downward) pointing triangles indicate positive (negative) trends. Trend magnitudes are proportional to the triangle sizes and green circles (pink outlines) indicate locally (globally) statistically-significant trends ($p < 0.05$). Results are shown only when $ny \geq 30$ years.

Supplementary Files

This is a list of supplementary files associated with this preprint. Click to download.

- SupplementaryInformation.pdf
- SupplementaryTable2.xlsx
- SupplementaryTable3.xlsx
- WHITimeSeries.xlsx